J. Fluid Mech. (1977), *vol.* 82, *part* 2, *pp.* 223–240
Printed in Great Britain

A contribution to an inviscid vortex-shedding model for an inclined flat plate in uniform flow

By MASARU KIYA AND MIKIO ARIE
Faculty of Engineering, Hokkaido University, Sapporo, 060 Japan

(Received 12 July 1976)

Unsteady separated flow behind an inclined flat plate is numerically studied through the use of the discrete-vortex approximation, in which the shear layers emanating from the edges of the plate are represented by an array of discrete vortices introduced into the flow field at appropriate time intervals at some fixed points near the edges of the plate. The strengths of the nascent vortices are chosen so as to satisfy the Kutta condition at the edges of the plate. Numerical calculations are performed for a plate at 60° incidence impulsively started from rest in an otherwise stationary incompressible fluid, by systematically changing the distance between the location of the nascent vortices and the edges of the plate. The temporal changes in the drag force, the rate of vorticity transport at both edges of the plate and the velocity of the separated shear layers are given together with the flow patterns behind the plate on the basis of this model. The results of the computation show that the vortex street behind the plate inclines as a whole towards the direction of the time-averaged lift force exerted on the plate. It is also predicted from the calculations that the vortex shedding at one edge of the plate will not occur at the mid-interval of the successive vortex shedding at the other edge. The predicted flow patterns are not inconsistent with a few experimental observations based on the flow-visualization technique.

1. Introduction

The main method of calculating unsteady fully separated flows over two-dimensional bluff bodies at sufficiently large Reynolds numbers makes use of a discrete-vortex model, in which the shear layers emanating from the separation points on the surface of the body are represented by an array of discrete vortices introduced into the flow field at appropriate time intervals at some points near the separation points. The motion of the shear layers in time is then approximated by the evolution of the arrays of discrete vortices. The limitations and usefulness of the discrete-vortex approximation were demonstrated by Clements & Maull (1975), who also gave an extensive list of the previous investigations in this category. One of the most crucial points in the calculation may be the determination of the position and strength of each new vortex introduced into the flow in the vicinity of the separation points. These vortices will hereafter be referred to as the nascent vortices.

This model was mainly applied in the past to the flow behind circular cylinders. However, since the separation points of the shear layers from the cylinder fluctuate in a manner which is not well understood as yet, the previous investigators had to make various assumptions about the separation points in their calculations of the flow. In

this sense the circular cylinder is not necessarily an appropriate shape with which to investigate the potentiality of the model of discrete-vortex approximation. This fact led some investigators to calculate the flow around bodies with fixed separation points for the purpose of obviating the need for any assumptions about the separation position. Clements (1973) and Clements & Maull (1975) made extensive studies of the flow behind a bluff plane-based body of semi-infinite length having right-angle corners between the sides and the rear face. Clements & Maull (1975) also applied the discrete-vortex model to a bluff-based body with suitable modifications to take account of the effects of base bleed, forced vortex shedding, a base cavity and a plane solid wall behind the base. Kuwahara (1973) and Sarpkaya (1975) were concerned with an inclined flat plate at various angles of attack.

The methods of Kuwahara and Sarpkaya use the Kutta condition to obtain a relation between the positions and strengths of the nascent vortices. Kuwahara introduced the nascent vortices at two fixed points near the edges of the plate, their strengths being determined from the Kutta condition. Therefore this method may be called the method of fixed positions of the nascent vortices and will hereafter be referred to as MFP. It should be noted that Clements & Maull (1975) also employed MFP in some cases, other calculations being performed by the $\partial\Gamma/\partial t = \frac{1}{2}U_s^2$ method, as they call it, where Γ and t will be defined just below and U_s is the velocity in the plane of the rear face of the body a short distance out from the separation point. Obviously the positions of the nascent vortices are the crucial parameters in MFP. Sarpkaya's procedure, on the other hand, determines the strengths of the nascent vortices from the relation

$$\partial\Gamma/\partial t = \tfrac{1}{2}\tilde{U}_{\mathrm{sh}}^2, \tag{1}$$

where Γ is the vorticity shed into the wake, t is the time and $\tilde{U}_{\mathrm{sh}}$ is interpreted as the velocity in the shear layers calculated by using the average of the transport velocities of four vortices in each shear layer. The positions of the nascent vortices are chosen so as to satisfy the Kutta condition at the edges of the plate and they can move slightly with time. As far as the positions of the nascent vortices are concerned, this method may be classified as the method of variable positions of the nascent vortices and will hereafter be referred to as MVP. The number of disposable parameters is reduced to a minimum in MVP and in this sense MVP may be superior to MFP. Moreover, Sarpkaya argues that the oscillation of the point of appearance of the nascent vortices is vital to the continuation of oscillations in resistance and is coupled with the manner in which the vortex sheets roll up. Sarpkaya also argues that MVP simulates in a satisfactory manner the mechanism of feedback from wake fluctuations to the fluctuations in the rate of circulation, while MFP does not.

However, it is the authors' opinion that there is still a problem connected with the relation (1) which is assumed in MVP. The rate at which the vorticity is shed into the wake is closely approximated by

$$\partial\Gamma/\partial t = \tfrac{1}{2}(\tilde{V}_{\mathrm{max}}^2 - \tilde{V}_{\mathrm{min}}^2) \simeq \tfrac{1}{2}\tilde{V}_{\mathrm{max}}^2, \tag{2}$$

where $\tilde{V}_{\mathrm{max}}$ and $\tilde{V}_{\mathrm{min}}$ represent the velocities at the *outer* and *inner* edges of the shear layer. Comparison of (1) with (2) reveals that MVP employs the assumption $\tilde{U}_{\mathrm{sh}} = \tilde{V}_{\mathrm{max}}$, which could not generally be acceptable in view of the velocity profile in the actual shear layers. Furthermore, Sarpkaya's argument that the oscillation of the positions of the nascent vortices is vital to the continuation of oscillations in resistance cannot

be taken as conclusive. It is true that the configuration and vorticity of the shear layers fluctuate in accordance with fluctuations in the wake. However, since the separation points on the flat plate are fixed at both edges, the fluctuation of the shear layers will not necessarily lead to the fluctuation of the positions of the nascent vortices. In this respect it is a pity that Clements (1973) and Clements & Maull (1975) treated a bluff body for which the drag force could not be defined. As will be shown later, a periodic variation of the drag force on an inclined flat plate can actually be obtained by means of MFP.

The results of Sarpkaya demonstrated in detail the kinematic and dynamic characteristics of the flow behind an inclined flat plate which can be calculated for various angles of attack on the basis of MVP, while the potentialities of MFP have not yet been studied to the same extent as those of MVP in this typical case of an inclined flat plate. This situation, together with the fact that MFP is much easier to apply than MVP is, may warrant detailed examination of the unsteady separated flow around an inclined flat plate on the basis of MFP. The computational results given in Kuwahara's paper are limited to the temporal variation of the drag coefficient of the flat plate in the incidence range 30–89° and to the evolution of the vortex pattern in the wake during an early stage of the flow development. An assessment of MFP would not be complete without the information cited below.

(i) The Strouhal number. As pointed out by Sarpkaya (1975), the oscillations of the drag force calculated by Kuwahara (1973) do not show any definite periodicity, which would be related to the periodic vortex shedding from the plate. It is conjectured that this result is caused by an improper replacement of vortex clusters by equivalent single vortices in Kuwahara's calculation.

(ii) Temporal variation of $\partial\Gamma/\partial t$. Since the mean velocity $V_{\max}$ at the outer edge of the shear layers is related to $\partial\Gamma/\partial t$ by $V_{\max} = (2\,\overline{\partial\Gamma/\partial t})^{\frac{1}{2}}$, where the overbar implies the mean value over one cycle of the periodic vortex shedding, the value of $\overline{\partial\Gamma/\partial t}$ gives a clue to estimating the back pressure of the plate. Moreover, the oscillation of $\partial\Gamma/\partial t$ will permit the determination of the Strouhal number.

(iii) The relation between the position of appearance of the nascent vortices and the resulting flow characteristics and forces. This relation can be found by systematically changing the distance between the separation point and the position of the nascent vortices.

(iv) Vortex patterns in the wake during the stage of steadily periodic vortex shedding. The periodic flow patterns cannot be predicted from vortex patterns in an early stage of the flow development such as those shown in Kuwahara (1973).

(v) The relation between the phase of the vortex shedding and the magnitude of the oscillating force exerted on the plate.

The main purpose of the present paper is to clarify the kinematic and dynamic characteristics of the flow over an inclined flat plate which can be calculated on the basis of MFP, with special reference to the characteristics described above in (i)–(v). Among the results obtained, it should be mentioned that MFP actually yields periodic variation of the drag force. It is also found that some aspects of the vortex pattern in early stages of the flow development show better agreement with the few experiments in the case of MFP than in the case of MVP.

2. Mathematical formulation of the model

The velocity of any one of the vortices is the sum of the two-dimensional irrotational potential flow around the plate and the velocity induced at the vortex position by all the other vortices. These velocities can conveniently be obtained by the introduction of a transformation plane in which the plate becomes a circle.

The transformation from the physical plane $z = x + iy$ to the transformed plane $Z = X + iY$ is given by

$$z = ie^{-i\alpha}(Z - a^2/Z), \tag{3}$$

where a and α are real constants. The velocity components in the x, y and X, Y directions will be denoted by u, v and U, V respectively. The circle of radius a with centre at the origin of the Z plane, i.e. $Z = ae^{i\theta}$ $(0 \leqslant \theta \leqslant 2\pi)$, is transformed into an inclined flat plate of length $4a$ in the physical plane described by

$$y = -x \tan \alpha. \tag{4}$$

If there exists a free stream in the direction of the x axis, the angle of attack of the plate will become α. The leading and trailing edges of the plate, i.e. S_1 and S_2, are then located at

$$z_{S_1} = -2ae^{-i\alpha}, \quad z_{S_2} = 2ae^{-i\alpha}, \tag{5}$$

which correspond to

$$Z_{S_1} = ai, \quad Z_{S_2} = -ai \tag{6}$$

in the transformed plane. In what follows, the suffixes 1 and 2 will refer to the leading and trailing edges of the plate. The two-dimensional irrotational potential flow around the plate is described by a complex flow potential W_u of the form

$$W_u = ie^{-i\alpha}U_\infty(Z - e^{2i\alpha}a^2/Z), \tag{7}$$

where U_∞ is the velocity of the approaching free stream.

The points S_1 and S_2 are the separation points of the flow over the plate, and the shear layers emanating from these points yield a distribution of vorticity behind the plate which is approximated by a system of rectilinear vortices in the discrete-vortex model. The vorticity shed from the leading edge is represented by vortices rotating clockwise (called S_1-vortices), while that shed from the trailing edge is represented by vortices rotating counterclockwise (called S_2-vortices). Let Γ_{1k} and Z_{1k} denote the circulation and location in the transformed plane of the kth S_1-vortex. Also let $-\Gamma_{2k}$ and Z_{2k} denote the circulation and location of the kth S_2-vortex. The complex flow potential $W_v^{(N)}$ which describes the flow induced by the S_1- and S_2-vortices is then given by

$$W_v^{(N)} = \sum_{k=1}^{N_1} i(2\pi)^{-1}\Gamma_{1k} \log\{(Z - Z_{1k})/(Z - a^2/Z_{1k}^*)\} - \sum_{k=1}^{N_2} i(2\pi)^{-1}\Gamma_{2k} \log\{(Z - Z_{2k})/(Z - a^2/Z_{2k}^*)\}, \tag{8}$$

where N_1 and N_2 are the numbers of S_1- and S_2-vortices in the flow field and an asterisk indicates a complex conjugate.

In MFP, another two vortices (nascent vortices) with strengths of Γ_{10} and $-\Gamma_{20}$ are introduced at the points Z_{10} and Z_{20}, which are located in the vicinity of the separation

points, in order to satisfy the Kutta condition. The complex velocity potential $W_v^{(0)}$ of the nascent vortices is given by

$$W_v^{(0)} = i(2\pi)^{-1}\Gamma_{10}\log\{(Z-Z_{10})/(Z-a^2/Z_{10}^*)\} - i(2\pi)^{-1}\Gamma_{20}\log\{(Z-Z_{20})/(Z-a^2/Z_{20}^*)\}. \tag{9}$$

The tangential separation at the edges of the plate (Kutta condition) can be realized by requiring

$$dW/dZ = 0 \quad \text{at} \quad Z = \pm ai, \tag{10}$$

where

$$W = W_u + W_v^{(N)} + W_v^{(0)}. \tag{11}$$

Equation (10) can be reduced to the following equations which permit determination of the strengths of the nascent vortices in MFP:

$$A_1(ai)\,\Gamma_{10} - A_2(ai)\,\Gamma_{20} = 2\pi B(ai), \tag{12a}$$

$$A_1(-ai)\,\Gamma_{10} - A_2(-ai)\,\Gamma_{20} = 2\pi B(-ai), \tag{12b}$$

where the functions A_1, A_2 and B are defined by

$$A_1(Z) = i\{(Z-Z_{10})^{-1} - (Z-a^2/Z_{10}^*)^{-1}\},$$

$$A_2(Z) = i\{(Z-Z_{20})^{-1} - (Z-a^2/Z_{20}^*)^{-1}\},$$

$$B(Z) = -\{(dW_u/dZ) + (dW_v^{(N)}/dZ)\}.$$

The velocity of the kth S_j-vortex, where $j = 1$ or 2, in the physical plane is given by

$$u_{jk} - iv_{jk} = \left(\frac{d}{dz}\{W - (-1)^{j+1}i(2\pi)^{-1}\Gamma_{jk}\log(z-z_{jk})\}\right)_{z=z_{jk}}. \tag{13}$$

In view of the relation obtained from (3),

$$z - z_{jk} = ie^{-i\alpha}(Z-Z_{jk})\,[1 + \{a^2/(ZZ_{jk})\}],$$

(13) can be written in the form

$$u_{jk} - iv_{jk} = -ie^{i\alpha}\frac{Z_{jk}^2}{Z_{jk}^2+a^2}(U_{jk} - iV_{jk}) + (-1)^{j+1}e^{i\alpha}\frac{\Gamma_{jk}}{2\pi}\frac{a^2 Z_{jk}}{(Z_{jk}^2+a^2)^2}, \tag{14}$$

where

$$U_{jk} - iV_{jk} = \left(\frac{d}{dZ}\{W - (-1)^{j+1}i(2\pi)^{-1}\Gamma_{jk}\log(Z-Z_{jk})\}\right)_{Z=Z_{jk}} \tag{15}$$

is the velocity of the kth S_j-vortex in the transformed plane.

The time development of the system of vortices is calculated from the relation

$$z_{jk}(t+\delta t) = z_{jk}(t) + \tfrac{1}{2}\{3(u_{jk}+iv_{jk})_t - (u_{jk}+iv_{jk})_{t-\delta t}\}\,\delta t + O(\delta t^3), \tag{16}$$

where δt is a small time increment. A time marching scheme of second-order accuracy is employed in this calculation in order to keep the accumulation of errors in moving the vortices as small as possible. Estimation of the accumulation of errors will be discussed in §3.† Movement of vortices in accordance with (16) will automatically

† A referee expressed concern over the accumulation of errors and the unstable perturbations that can develop in any time marching scheme. An order-of-magnitude estimation of the accumulation of errors may be possible, while the onset of the unstable perturbations could not be predicted *a priori*. However, the results of the computation seem to show that significant unstable perturbations did not occur on large scales in the time marching scheme employed in this investigation.

yield periodic vortex shedding from the edges of the plate and the resulting formation of a Kármán vortex street behind the plate.

The oscillating forces exerted on the plate can be calculated from the generalized Blasius theorem

$$\tilde{D}-i\tilde{L}=\frac{i}{2}\rho\oint(dW/dz)^2\,dz+i\rho\frac{\partial}{\partial t}\oint W^*\,dz^*, \tag{17}$$

in which $\tilde{D}$ and $\tilde{L}$ represent the drag and lift forces on the plate and ρ is the density of the fluid. On substituting (11) into (17) and carrying out the integrations, one finally obtains

$$\begin{aligned}\tilde{D}-i\tilde{L}=&\sum_{j=1}^{2}(-1)^{j+1}i\rho\sum_{k=0}^{N_j}\Gamma_{jk}(u_{jk}-iv_{jk})\\&-\sum_{j=1}^{2}(-1)^{j+1}i\rho a^2\sum_{k=0}^{N_j}\Gamma_{jk}\left(e^{2i\alpha}\frac{u_{jk}+iv_{jk}}{Z_{jk}^2+a^2}+\frac{u_{jk}-iv_{jk}}{Z_{jk}^{*2}+a^2}\right).\end{aligned} \tag{18}$$

As demonstrated by Sarpkaya (1975), there is no force acting along the plate since the velocities at both the leading and the trailing edge are rendered finite by satisfying the Kutta condition at both edges. Accordingly, one will have

$$\tilde{D}/\tilde{L}=\tan\alpha. \tag{19}$$

The forces $\tilde{D}$ and $\tilde{L}$ may be expressed in terms of the drag and lift coefficient, defined as

$$(\tilde{C}_D,\tilde{C}_L)=(\tilde{D},\tilde{L})/\{\tfrac{1}{2}\rho U_\infty^2(4a)\}. \tag{20}$$

3. Numerical procedure

In the present calculation the fluid is assumed to be set in motion impulsively from rest. This situation can be realized experimentally by moving the plate impulsively in an otherwise stationary fluid. Since the actual flow is expected to leave the edges of the plate tangentially, it is reasonable to choose the positions of the nascent vortices in the plane of the plate and at a short distance downstream of the separation points. The same choice of the positions of the nascent vortices was also made by Kuwahara (1973), Sarpkaya (1975) and Clements & Maull (1975). In the present calculation the distance a_s between the separation point and the location of a nascent vortex is taken to be the same at both the leading and the trailing edge of the plate. Although the distance a_s could be different at the two edges, the same distance is employed here in the interests of making the number of disposable parameters as small as possible.

Since a large number of vortices exist in the flow field, it is probable that some vortices attain small separations and produce large velocities at each other's positions because of the absence of viscosity. This was avoided in the present calculation by employing a stream function of the following form, which was originally suggested by Chorin (1973):

$$\psi_\sigma=\begin{cases}(2\pi)^{-1}\Gamma\log r & (r>\sigma),\\ (2\pi)^{-1}\Gamma(r/\sigma) & (r\leqslant\sigma)\end{cases} \tag{21}$$

for each vortex. In this equation Γ is the circulation of the vortex, r is the radial distance measured from the centre of the vortex and σ is a cut-off length whose introduction is analogous to the introduction of a small viscosity which allows the vorticity in a point vortex to diffuse. It is important to note that the introduction of a cut-off

does not affect the mutual interaction of distant portions of the vortex sheets. Furthermore, Chorin (1973) argues that the results of the calculation are not sensitive to the exact choice of ψ_σ for $r \leqslant \sigma$. The stream function ψ_σ yields a circumferential velocity v_θ of the form

$$v_\theta = \begin{cases} (2\pi r)^{-1}\Gamma & (r > \sigma), \\ (2\pi\sigma)^{-1}\Gamma & (r \leqslant \sigma). \end{cases} \tag{22}$$

The value of σ was chosen as $0{\cdot}05(2a)$ by taking into account the values of similar parameters employed by previous investigators, including Gerrard (1967), Clements (1973) and Sarpkaya (1975). Coalescence of vortices in the manner which was described by Clements (1973) and Sarpkaya (1975) is not employed in the present calculation. It should be noted here that the discrete-vortex approximation cannot be expected to produce a meaningful model of the fine-structure of the rolled-up vortex sheets even if the procedure described by (22) is employed in the movement of individual vortices in order to control the instabilities caused by the presence of the singularity at each potential vortex. However, excessive instabilities in the movement of vortices can be avoided by this procedure. The point is that one can obtain from the discrete-vortex model the general characteristics of large unsteady flow regions such as the clusters of vortices formed behind the plate.

It is also probable that individual vortices approach too close to the rear surface of the plate and this causes them to have unreasonably high velocities along the plate owing to the presence of the image vortices within the circle in the transformed plane. These vortices were removed from the flow field whenever they came nearer to the rear face of the plate than a distance of $0{\cdot}05(2a)$.

The time step δt was determined by repeating a few calculations with a single program with only the time step changed and in addition by referring to the results of the previous investigators already mentioned. The time step finally employed in the present calculation is $\delta t = \delta t_0 = 0{\cdot}08(2a/U_\infty)$. The kinematic and dynamic characteristics of the flow thus calculated showed only an insignificant difference from those obtained with $\delta t = \frac{1}{2}\delta t_0$. In passing it should be mentioned that the optimum time step depends on the interval between the introduction of the new vortices into the wake, which will be denoted by δt_i. The very small time step $\delta t = \frac{1}{4}\delta t_0$ adopted by Sarpkaya (1975) was necessary because the interval $\delta t_i = 5\delta t$ was selected in his calculation. The value $\delta t_i = 2\delta t$ was adopted by Clements (1973) and also in the present calculation. This procedure is required in order to keep the computation time within reasonable bounds.

In view of the computation time, it was also necessary to combine the point vortices in a given vortex cluster into an equivalent single vortex whose strength was the sum of the individual strengths and whose position was the centre of vorticity of the cluster. This procedure, which was originally adopted by Chaplin (1973) and Clements (1973), was used when a cluster passed beyond a downstream distance of about $x/(2a) = 4$.

The accumulation of errors in moving the vortices in accordance with (16) will now be considered. As will be shown later in figure 1, hydrodynamic characteristics of the plate such as the drag force and the rate of vorticity shedding from the edges exhibit definite periodicities with respect to time, which are the result of the periodic vortex shedding from the plate. Since the shapes of these curves are little influenced by the replacement of the clusters of vortices by an equivalent single vortex in the region beyond $x/(2a) = 4$, it might be reasonable to assume that the fine-structures of

α	$U_\infty \delta t/(2a)$	$U_\infty \delta t_i/(2a)$	$\sigma/(2a)$	$a_s/(2a)$				
60°	0·08	0·16	0·05	0·005	0·009	0·0125	0·025	0·05

TABLE 1. Parameters employed in the present calculation.

the vortex clusters in this region have only a negligible influence on the hydrodynamic characteristics of the plate. This assumption will imply that the unsteady hydrodynamic characteristics of the plate are primarily determined by the structures of the pair of vortex clusters existing just behind the plate. Accordingly, it is sufficient to consider the accumulation of errors in one cycle of the periodic vortex shedding. Let τ denote the period of the vortex shedding. The accumulated error in the position of each point vortex, say δz, is then estimated to be of the order of

$$\delta z/(2a) = O[(\tau/\delta t_0)\{U_\infty \delta t_0/(2a)\}^3].$$

Since $\tau \simeq 14(2a/U_\infty)$ (see figure 1) and $\delta t_0 = 0{\cdot}08(2a/U_\infty)$, one has

$$\delta z/(2a) = O(0{\cdot}09),$$

which, in the authors' opinion, will not be large enough significantly to affect the form of the vortex-cluster formation.

4. Discussion of numerical results

Computations were made for the single angle of attack $\alpha = 60°$ by systematically changing the distance a_s between the separation points and the positions of the nascent vortices. The parameters used in the calculations are summarized in table 1. In the authors' opinion, the fact that only one angle of attack is treated in this study will not necessarily hinder one from understanding the characteristics of the flow calculated by MFP. The detailed discussion of results will be confined to the case $a_s/(2a) = 0{\cdot}0125$ in the interests of space, and additional comments will be presented for other values of a_s.

Figure 1 shows the temporal variation of the drag coefficient, the rate of shedding of vorticity into the shear layers emanating from the leading and trailing edges of the plate and the convective velocities of the shear layers, defined in the same way as Sarpkaya (1975). All of the curves shown in figure 1 exhibit definite periodicities in accordance with the periodic vortex shedding from the plate. The periodicity in the drag force is particularly noteworthy in view of the fact that Kuwahara (1973) could not obtain any definite periodicity in his calculation by MFP. The results of Kuwahara led Sarpkaya to conclude that the oscillation of the point of nascent vortices is vital to the continuation of oscillation in the drag force even in the case of an inclined flat plate. Now it is obvious that the absence of periodic changes in the drag force in Kuwahara's calculation may have its origin in the improper procedure of combining the point vortices into an equivalent single vortex and is not an intrinsic fault of MFP. In this respect the work of Chaplin (1973), who calculated the unsteady separated flow around a circular cylinder by introducing the nascent vortices at some fixed points near the surface of the cylinder should be mentioned. Since he obtained a periodic wave form

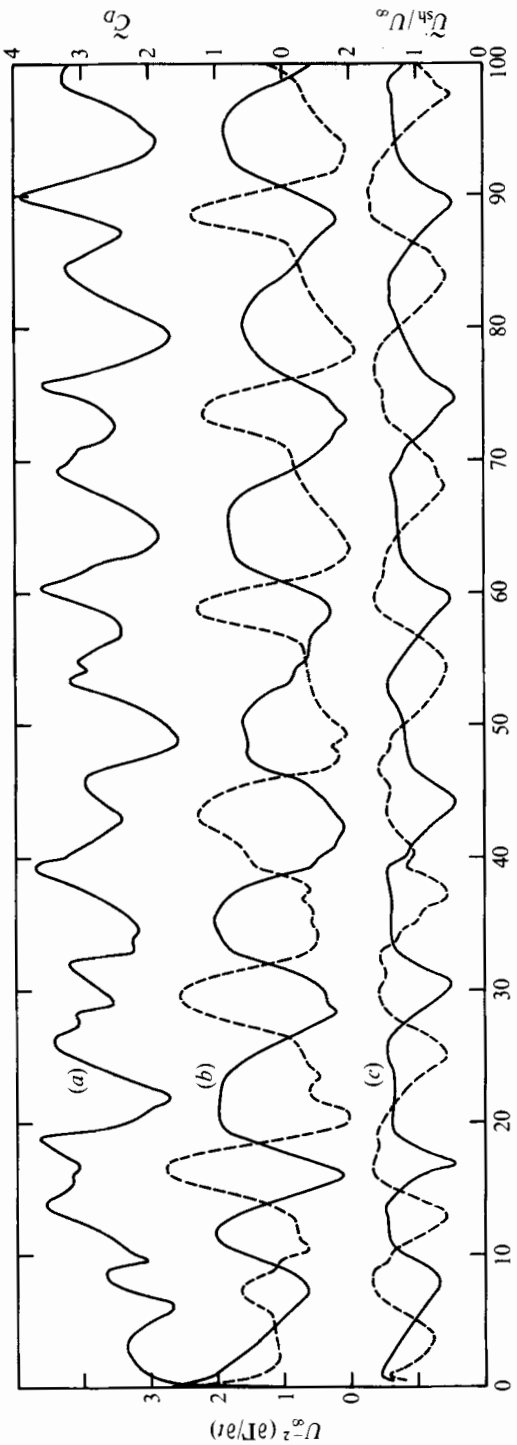

FIGURE 1. Wave forms of (*a*) the drag coefficient $\tilde{C}_D$, (*b*) the rate of shedding $U_\infty^{-2}\,\partial\Gamma/\partial t$ of vorticity into shear layers emanating from the leading and trailing edges of the plate and (*c*) the convective velocity $\tilde{U}_{sh}/U_\infty$ of the shear layers. $\alpha = 60°$, $a_s/(2a) = 0{\cdot}0125$. ——, leading edge; – – –, trailing edge.

for the drag force, Sarpkaya's argument about the relation between the location of the nascent vortices and the drag-force oscillation cannot be justified.

The maximum values of the drag coefficient are seen to occur at the times when the convective velocity $\bar{U}_{\rm sh}$ of the shear layers approximately takes its maximum and minimum values, while in Sarpkaya's calculation based on MVP the maxima of $\bar{C}_D$ appear when $\partial\Gamma/\partial t$ approximately attains its maxima and minima. Since the relation (1) is assumed in MVP, the phase relation between the drag force and the convective velocity of the shear layers is found to be the same in both MFP and MVP. It may be noted that $(\partial\Gamma/\partial t)_1$ and $(\partial\Gamma/\partial t)_2$ as calculated by MFP take approximately the same values when the maxima of the drag coefficient appear. In view of (2), this fact implies that the velocities at the outer edges of the shear layers emanating from both edges of the plate become approximately the same at the time of the maxima of $\bar{C}_D$. Since it is difficult to measure the wave form of $\partial\Gamma/\partial t$ or the convective velocity of the shear layers, the phase relation just described could not be compared with experiments.

The wave forms of the drag coefficient and the rate of shedding of vorticity calculated by Sarpkaya on the basis of MVP are closely sinusoidal in the stages of steadily periodic vortex shedding behind the plate. However, as will be seen in figure 1, the wave forms of the corresponding quantities obtained by MFP are not sinusoidal and amplitudes are much larger than those calculated by MVP. Since no experimental information about the amplitude of the unsteady drag force exerted on the plate at high Reynolds numbers is available to the authors, use will be made of a numerical solution of the Navier–Stokes equations which was obtained by Lugt & Haussling (1974) for a slender elliptical cylinder with an incidence of 45° to the approaching uniform stream, the Reynolds number based on the major diameter of the cylinder being 200. Even this sort of information, in the authors' opinion, will give some clue to the nature of the unsteady wave forms of the relevant hydrodynamic properties at much higher Reynolds numbers. The wave form of the drag coefficient plotted against time is neither sinusoidal in their calculation nor very close to that predicted by MFP. The peak-to-peak amplitude of the drag coefficient calculated by Lugt & Haussling is about 0·3 times the mean drag coefficient, while the ratio is 0·6 ($\alpha = 60°$, $a_s/(2a) = 0{\cdot}0125$) for MFP and 0·1 ($\alpha = 50°$) for MVP. It is hoped that unsteady measurements in the future will reveal experimentally the wave forms of the oscillating drag force exerted on the plate.

It is plausible that the large amplitude of the drag coefficient is due to the failure of the model to produce cancellation of vorticity during the formation of vortices. Consequently, the strengths of the vortex clusters formed in this model are larger and create greater fluctuating forces than those obtained by Sarpkaya and Lugt & Haussling. The inaccuracy of the present model in this respect may be primarily a result of the lack of proper representation of viscous diffusion and turbulent entrainment in the shear layers.

A general trend of the wave forms of $\bar{C}_D$, $\partial\Gamma/\partial t$ and $\bar{U}_{\rm sh}$ like that shown in figure 1 is also found in all calculations for other values of the parameter a_s except for the case of $a_s/(2a) = 0{\cdot}005$, in which periodic wave forms could not be obtained by MFP. It is observed that the amplitudes of the wave forms increase with increasing a_s. The dependence of the mean values over one cycle of vortex shedding on the parameter a_s will be discussed later. It may be worth while to mention that the relation (19) is satisfied with a very high accuracy.

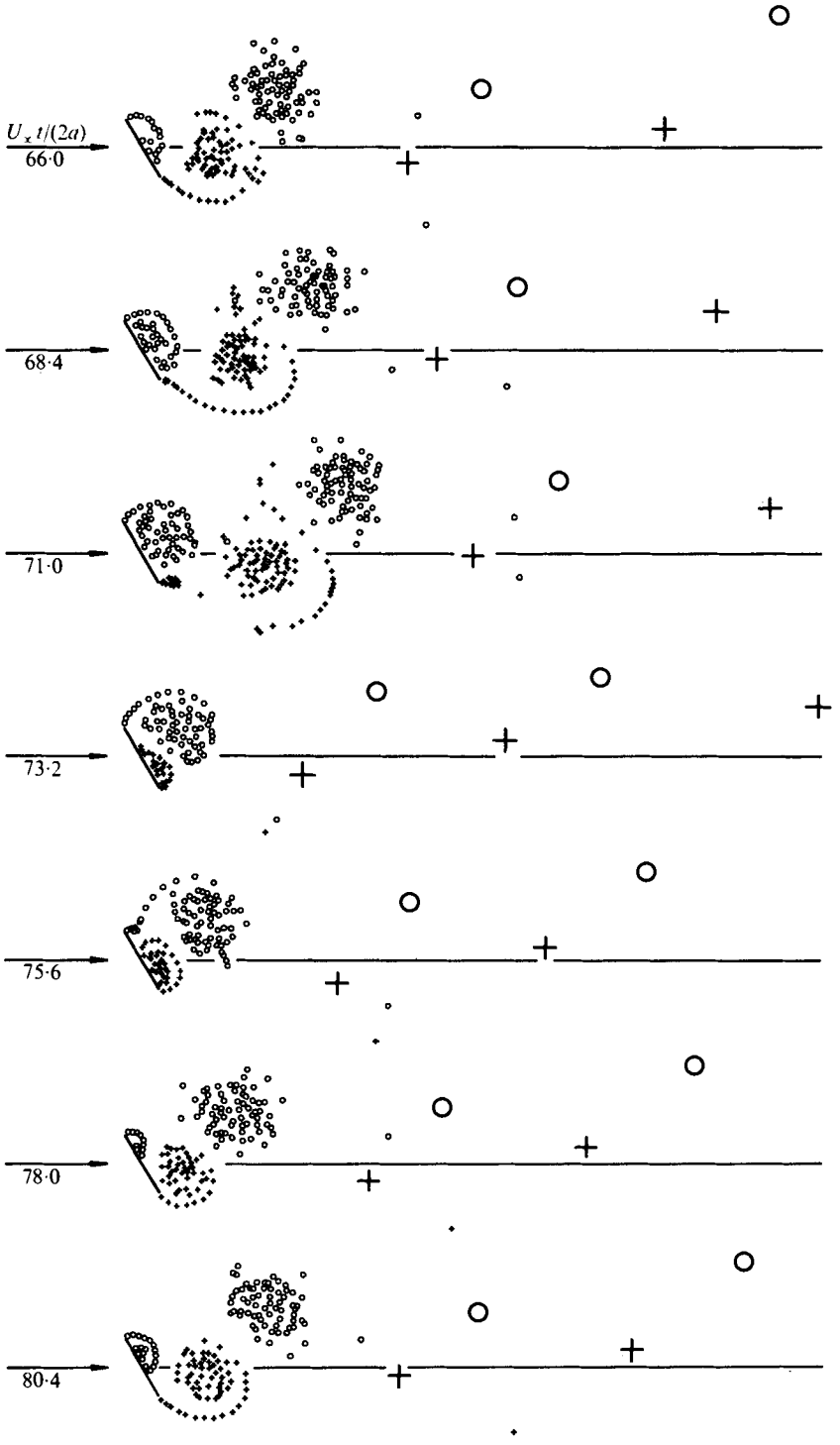

FIGURE 2. Vortex patterns over one full cycle of steadily periodic flow. ○, clockwise vortices; +, counterclockwise vortices. $\alpha = 60°$, $a_s/(2a) = 0{\cdot}0125$.

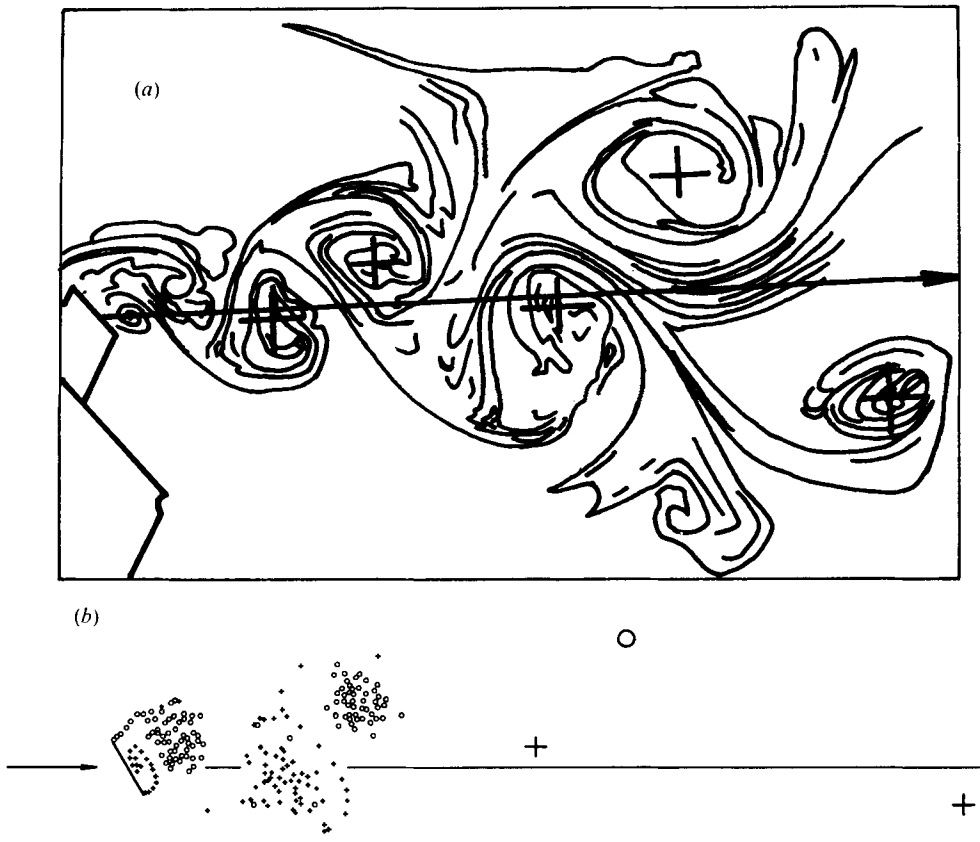

FIGURE 3. (*a*) Sketch of vortex pattern behind the plate taken from figure 5 of Sarpkaya (1975). Approximate locations of vortices and the free-stream direction are indicated by the plus sign and an arrow respectively; $\alpha = 50°$, $t = 37{\cdot}0(2a/U_\infty)$. (*b*) Vortex arrangements calculated by MFP; $\alpha = 60°$, $t = 30{\cdot}6(2a/U_\infty)$.

Figure 2 shows the evolution of the wake over one full cycle of steadily periodic vortex shedding and the replacement of vortex clusters by equivalent single vortices. It is evident that the vortex street behind the plate inclines as a whole towards the time-averaged lift force exerted on the plate. The same type of vortex pattern was also obtained for other values of a_s. The inclination of the vortex street may be related to the phase difference between the vortex shedding from the leading edge and that from the trailing edge. Let the phase difference between two successive vortex sheddings from the leading edge be defined as 2π. In an ordinary Kármán vortex street such as that formed behind a two-dimensional circular cylinder, the vortex shedding from the trailing edge will take place at a phase angle of π. However, as may be clearly seen in the wave forms of $\partial\Gamma/\partial t$ shown in figure 1, the calculated vortex shedding from the trailing edge occurs at a phase angle less than π. In this connexion the analysis of Maue (1940), which presented a generalization of the Kármán vortex street, should be mentioned. Maue considered a staggered vortex street in which each vortex in one row was not exactly opposite to the centre of the interval between two consecutive vortices in the other row and demonstrated that this vortex arrangement was stable with respect to two-dimensional infinitesimal disturbances. The velocity induced

at any vortex in Maue's vortex street by all the other vortices has components both parallel and normal to the approaching flow, so that the axis of Maue's vortex street is not parallel but inclined to the direction of the flow.

As far as the authors are aware, no experimental verification of Maue's vortex street has yet been reported in the literature. Struck by the results of the calculation, the authors re-examined the experimental data available. Figure 3(*a*) shows a sketch of the vortex pattern behind a plate at 50° incidence at a time $t = 37{\cdot}0(2a/U_\infty)$ after the impulsive start of flow, which was taken from a photograph by Sarpkaya (1975). Approximate locations of the vortices and the approximate direction of the free stream are indicated in figure 3(*a*). The calculated flow pattern which approximately corresponds to the same phase of vortex formation as the experimental one is shown in figure 3(*b*). A comparison of figure 3(*a*) with figure 3(*b*) reveals that the agreement between the positions of the vortex clusters predicted numerically and those observed experimentally is fairly good except for the rightmost cluster, especially with regard to the inclination of the axis of the vortex street and the phase difference in the vortex shedding from the leading and trailing edges of the plate described above. It should be pointed out that the said inclination of the vortex-street axis and phase difference in the vortex shedding are not seen in the vortex patterns calculated by Sarpkaya through the use of MVP. As further information about the vortex patterns in earlier stages of the development of the flow, figures 4 and 5 (plates 1 and 2) show photographs of the vortex patterns behind an inclined flat plate at incidences of $\alpha = 50°$ and 60° which were taken by Takahashi (1976) by means of flow visualization with aluminium powder. Although the time elapsed since the impulsive start of the flow cannot be identified in this experiment, the rightmost vortices on the lower side are the first vortices shed into the wake for each angle of attack. Both inclination of the vortex-street axis and a phase difference in the vortex shedding may be observed in these photographs, especially in the case $\alpha = 50°$.

Figure 6 (plate 3) shows a vortex pattern in the wake behind a plate at $\alpha = 60°$ in which the vortex shedding is believed to be steadily periodic (Takahashi 1976). Although the inclination of the vortex-street axis may be less clear in this case than in figures 2, 3(*a*), 4 and 5, it is not necessarily impossible that a slight inclination exists. On the other hand, the aforementioned phase difference in the vortex shedding between the leading and trailing edges of the plate may be more clearly observed. However, since these properties are not significant enough to endure critical eyes, it is possible to say that they were brought about by some undefined perturbations to the vortex street. It should be remarked here that the phase difference in the vortex shedding and the inclination of the vortex-street axis may have their origin in the use of the same distance a_s of the nascent vortices from both the leading and trailing edges of the plate in the present calculation. This situation will explain why the results of Sarpkaya (1975) did not show the said properties related to the vortex shedding, because the location of nascent vortices is adjusted to satisfy the Kutta condition and slightly changes with time, according to the various stages of the formation of the vortex clusters. However, what is shown by the flow-visualization photographs deserves attention, and it is hoped that more detailed experimental studies in the future will be made to check the predictions of the present calculation.

Despite the absence of turbulent entrainment in the discrete-vortex model, the length of the formation region (Gerrard 1966) suggested by figure 2 is certainly much

$a_s/(2a)$	0·005	0·009	0·0125	0·025	0·05
C_D	1·68	2·38	2·66	3·40	3·72
$U_\infty^{-2}\overline{(\partial\Gamma/\partial t)_1}$	1·02	0·90	0·97	1·26	1·41
$U_\infty^{-2}\overline{(\partial\Gamma/\partial t)_2}$	1·04	0·78	0·90	1·19	1·08
$U_\infty^{-2}\overline{(\partial\Gamma/\partial t)_m}$	1·03	0·84	0·94	1·23	1·24
V_{max}/U_∞	1·43	1·30	1·37	1·57	1·58
C_{pb}	−1·04	−0·69	−0·88	−1·46	−1·50
U_{sh}/U_∞	—	—	1·14	—	—
St	—	0·14	0·14	0·13	0·11

TABLE 2. Summary of main results of the present calculation.

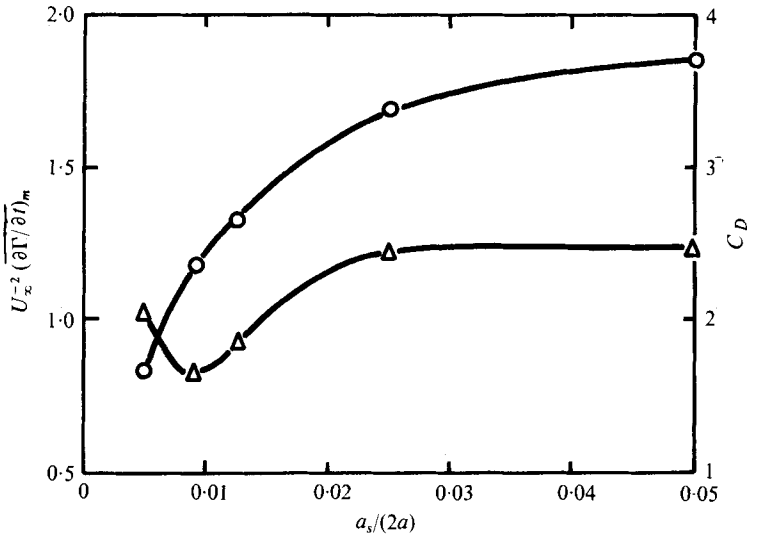

FIGURE 7. Variation of time-averaged drag coefficient C_D and the rate of shedding $U_\infty^{-2}\overline{(\partial\Gamma/\partial t)_m}$ of vorticity into shear layers with respect to a_s. $\alpha = 60°$. △, C_D; ○, $U_\infty^{-2}\overline{(\partial\Gamma/\partial t)_m}$.

smaller than that which can be estimated from the few flow-visualization photographs for a normal flat plate (Fage & Johansen 1927; Goldstein, 1965, § 241). This may result from the sensitivity of the separated shear layers to perturbations, which is increased by representation of the layers by a single line of potential vortices. Each shear layer is therefore less stable in position and more easily deflected inwards by the cross-flow associated with the previously growing vortex of opposite sign. Consequently, the shear layers cross the wake axis close to the plate and the formation length becomes unrealistically small.

The effects of the parameter a_s on the time-averaged characteristics of the flow around the plate over one cycle of steadily periodic vortex shedding will now be described. Table 2 summarizes the main results, while figure 7 shows the variation of the time-averaged drag coefficient C_D and the vorticity shedding rate $\overline{(\partial\Gamma/\partial t)_m}$ with respect to a_s, where the overbar implies the mean value and the suffix m the arithmetic average of the values at the leading and trailing edges of the plate. In the range of the parameter a_s employed in the present calculation, the mean drag coefficient C_D

monotonically decreases with decreasing a_s. Since the value of C_D obtained experimentally for $\alpha = 60°$ by Fage & Johansen (1927) is 1·5, the results obtained numerically by MFP are larger than the experimental one by factors of from 1·1 ($a_s/(2a) = 0{\cdot}005$) to 2·5 ($a_s/(2a) = 0{\cdot}05$). In this connexion it should be remarked that the mean drag coefficient calculated for $\alpha = 60°$ by Sarpkaya (1975) was about 25% larger than that obtained experimentally. Accordingly in this respect MVP yields better agreement with experiments than MFP does, although a considerable difference still exists between the calculated results and experiments even in the case of MVP. The larger deviation from experiments of the mean drag coefficient in MFP may be explained by larger accumulation of vorticity in the vortex clusters formed behind the plate. As an example, consider the case $a_s/(2a) = 0{\cdot}0125$ in table 2. The Strouhal number of vortex shedding, which will be discussed again later, is found to be 0·14 for MFP, while that for MVP is 0·178. Since the value of $U_\infty^{-2}\overline{(\partial\Gamma/\partial t)}_m$ is 0·94 for MFP and 0·99 for MVP, the accumulation of vorticity in a typical vortex cluster will be larger in MFP by a factor of $(0{\cdot}94/0{\cdot}99)(0{\cdot}178/0{\cdot}14) = 1{\cdot}21$ than in MVP. This factor could be compared to the ratio of the mean drag coefficients obtained by MFP and MVP, viz. $2{\cdot}66/1{\cdot}95 = 1{\cdot}36$ (see table 1 of Sarpkaya 1975). In fact Sarpkaya mentions that an appropriate reduction in the strengths of the vortices, particularly in the near wake, does bring about a reduction in the mean drag coefficient.

As may be seen in figure 7, the rate of shedding of vorticity $\overline{(\partial\Gamma/\partial t)}_m$ attains a minimum in the neighbourhood of $a_s/(2a) = 0{\cdot}09$ and becomes practically constant in the range $a_s/(2a) \geqslant 0{\cdot}025$. The time-averaged value of the velocities at the outer edges of the shear layers calculated from $V_{\max} = (\overline{2\,\partial\Gamma/\partial t})_m^{\frac{1}{2}}$ is $1{\cdot}37U_\infty$ when $a_s/(2a) = 0{\cdot}0125$. This value is only 3% smaller than that ($V_{\max} = 1{\cdot}41U_\infty$) measured by Fage & Johansen (1927). As remarked earlier, $V_{\max}$ is not equal to the mean convective velocity of the shear layers U_{sh_m} in MFP, while it is in MVP. U_{sh_m} is found to be $1{\cdot}14U_\infty$ in the case $a_s/(2a) = 0{\cdot}0125$, which is about 17% smaller than $V_{\max}$. The absence of figures in the last column but one of table 2 except for $a_s/(2a) = 0{\cdot}0125$ was caused by the fact that the corresponding data on magnetic tape had been eliminated at the time of the calculation of U_{sh_m}.

If it is assumed that the total kinetic energy at the outer boundary of the shear layers is equal to that in the undisturbed stream and that the pressure throughout the shear layers is the same as that at the base of the plate, the time-averaged base-pressure coefficient can be written as

$$C_{pb} = 1 - (V_{\max}/U_\infty)^2, \tag{23}$$

which is equivalent to the relation $C_{pb} = 1 - 2U_\infty^{-2}\,\overline{\partial\Gamma/\partial t}$ employed in Clements & Maull (1975). The values of C_{pb} calculated from this equation are included in table 2. Since the experimental base-pressure coefficient obtained by Fage & Johansen (1927) is $-1{\cdot}33$ for $\alpha = 60°$, MFP is expected to yield the same value of C_{pb} somewhere in the range of $a_s/(2a)$ between 0·0125 and 0·025. It may be worth mentioning here that the value of $V_{\max}/U_\infty$ determined from the experimental back pressure of Fage & Johansen is 1·53 for $\alpha = 60°$, while velocity measurements yield $V_{\max}/U_\infty = 1{\cdot}41$ as described just above, which corresponds to $C_{pb} \simeq -1{\cdot}0$ in view of (23). This experimental evidence implies that the theoretical value of $V_{\max}/U_\infty$ should be compared with $(1 - C_{pb})^{\frac{1}{2}}$, in which C_{pb} is the experimental base-pressure coefficient. In this respect

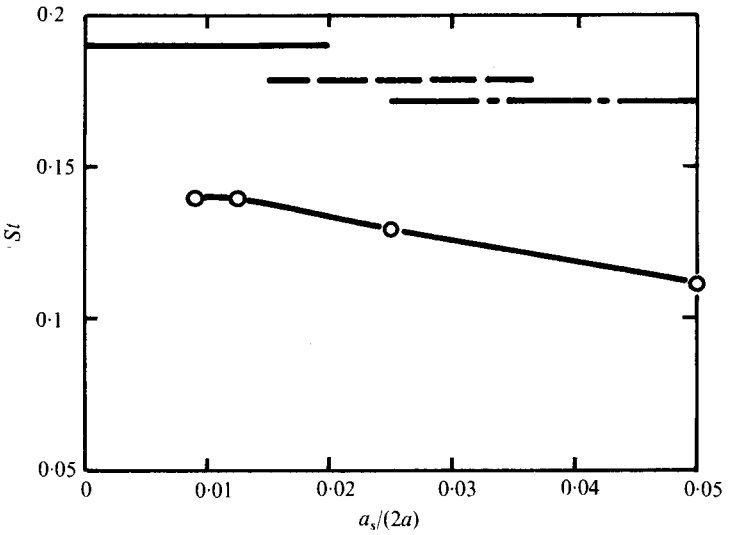

FIGURE 8. Variation of Strouhal number St with a_s ($\alpha = 60°$). —○—, present calculation; —— $St = 0{\cdot}190$, experiment by Abernathy (1962); – – –, $St = 0{\cdot}178$, calculation by Sarpkaya (1975); ———, $St = 0{\cdot}171$, experiment by Fage & Johansen (1927). Note that the abscissa has no meaning for the last three curves.

considerable errors still exist in the values of $V_{\max}/U_\infty$ calculated by MFP and MVP, in which $V_{\max}/U_\infty$ was found to be 1·41 for all angles of attack larger than 50°. The inaccuracy of the models is caused by the lack of proper representation of viscous diffusion and turbulent entrainment in the shear layers.

Since the periodicity of $\partial\Gamma/\partial t$ is quite significant as may be seen in figure 1, the Strouhal number St, defined by

$$St = 4af/U_\infty, \tag{24}$$

where f is the frequency of vortex shedding, can easily be calculated and the results are also included in table 2. Figure 8 shows the variation of St with respect to a_s. The calculated Strouhal number is seen to be almost constant and equal to 0·14 in the range $0{\cdot}009 \leqslant a_s/(2a) \leqslant 0{\cdot}0125$. The Strouhal numbers obtained experimentally for $\alpha = 60°$ are 0·171 (Fage & Johansen 1927) and 0·190 (Abernathy 1962), the tunnel-height to plate-chord constriction ratio being about 14 in both cases. The calculated values of St are thus less than the experimental ones by 22–36%. On the other hand, Sarpkaya (1975) obtained $St = 0{\cdot}178$ by means of MVP. Since the mechanism which determines the Strouhal number in the discrete-vortex model is not evident to the authors, the difference in St between MFP and MVP is not clear. However, it is possible that the constancy of the locations of the nascent vortices destroys some aspects of the manner in which the vortex sheets roll up, as suggested by Sarpkaya (1975).

The present calculation by MFP failed to yield definite periodicities in the wave forms of $\partial\Gamma/\partial t$ and $\tilde{C}_D$ when $a_s/(2a) = 0{\cdot}005$. Furthermore, in this case the calculated vortex clusters are much less coherent than those for other values of a_s, and in addition their positions are in poor agreement with the experimental observations. These facts may suggest that the distance $a_s = 0{\cdot}005(2a)$ is too small for calculation by MFP. On the other hand, it is quite natural to expect that an upper limit on a_s will exist. Table 2 shows that one cannot obtain a single value of a_s which yields satisfactory results for

all the hydrodynamic characteristics of the plate. Consequently an optimum value of a_s should be determined according to the information which is required. In view of the values of C_D, $V_{\max}$ and St shown in table 2, the two distances $a_s/(2a) = 0{\cdot}025$ and $0{\cdot}05$ may be judged to be too large. If reasonable results for the Strouhal number and the nature of the vortex-cluster formation are to be obtained, the distance a_s should be in the range

$$0{\cdot}005 < a_s/(2a) \leqslant 0{\cdot}0125. \tag{25}$$

In this connexion, the results of Clements & Maull (1975), who investigated the vortex shedding behind a square-based body by MFP, deserve attention. Choosing the positions of the nascent vortices in the planes of the body and at a short distance downstream of the separation points, they discovered that, if it was at a distance of between $0{\cdot}01$ and $0{\cdot}03$ times half the base height, the exact position of the nascent vortices did not affect the Strouhal number of the vortex shedding, nor the nature of vortex-cluster formation. Therefore their optimum range of the distance overlaps that described by (25). It is possible that the appropriate range of a_s will depend on the time step δt. Nevertheless no detailed examination of this point was made in the present study.

5. Conclusions

In the present paper the vortex shedding behind an inclined flat plate has been numerically studied through the use of the discrete-vortex approximation, in which the shear layers emanating from the leading and trailing edges of the plate are represented by an array of discrete vortices introduced into the wake at appropriate time intervals at some fixed points near the edges of the plate. The positions of appearance of the nascent vortices were chosen in the plane of the plate and at a short distance downstream of the separation points. The strengths of the nascent vortices were determined from the Kutta condition. Numerical calculations were performed for an inclined plate at 60° incidence set in motion impulsively from rest by systematically changing the distance between the positions of appearance of the nascent vortices and the edges of the plate. The results were compared with the similar calculations by Kuwahara (1973) and Sarpkaya (1975).

The main results can be summarized as follows.

(i) The distance a_s between the position of the nascent vortices and the edges of the plate should be in the range $0{\cdot}005 < a_s/(2a) \leqslant 0{\cdot}0125$, where $2a$ is the half-length of the plate, in order that this distance does not affect either the Strouhal number of vortex shedding or the nature of vortex-cluster formation.

(ii) The calculated Strouhal number of steadily periodic vortex shedding behind the plate takes a constant value of about $0{\cdot}14$ in the above range of a_s, which is smaller than the experimental values by 22–36%.

(iii) In the range of a_s described in (i), the time-averaged drag coefficient of the plate over one cycle of steadily periodic vortex shedding monotonically increases with increasing a_s, and is about 70% higher than that obtained experimentally when $a_s/(2a) = 0{\cdot}0125$.

(iv) The steadily periodic wave form of the drag force can be obtained by a discrete-vortex approximation in which the positions of appearance of the nascent vortices are fixed in the vicinity of both edges of the plate. Accordingly, the argument of

Sarpkaya (1975) that oscillation of the point of appearance of the nascent vortices is essential to the continuation of oscillations in the drag force is not justified.

(v) The present computation predicts that a vortex will not be shed from one edge of the plate at the mid-interval between two consecutive vortices shed from the other edge of the plate. In accordance with this fact, the calculated vortex street behind the plate inclines as a whole towards the side of the time-averaged lift force exerted on the plate. These predictions are found to be not inconsistent with a few flow-visualization photographs taken at earlier stages of the flow development. The results of the calculation by Sarpkaya (1975) do not show the aforementioned phase difference in the vortex shedding nor inclination of the vortex-street axis.

(vi) With regard to the predictions of the Strouhal number and the drag coefficient, the method of Sarpkaya yields better results than that with a fixed point of introduction of the nascent vortices considered in this study.

The authors are grateful to a referee for helpful comments which have led to an improved discussion of the paper.

REFERENCES

ABERNATHY, F. H. 1962 Flow over an inclined flat plate. *J. Basic Engng, Trans. A.S.M.E.* D **84**, 380.

CHAPLIN, J. R. 1973 Computer model of vortex shedding from a cylinder. *J. Hydraul. Div., Proc. A.S.C.E.* HY **1**, 155.

CHORIN, A. J. 1973 Numerical study of slightly viscous fluid. *J. Fluid Mech.* **57**, 785.

CLEMENTS, R. R. 1973 An inviscid model of two-dimensional vortex shedding. *J. Fluid Mech.* **57**, 321.

CLEMENTS, R. R. & MAULL, D. J. 1975 The representation of sheets of vorticity by discrete vortices. *Prog. Aerospace Sci.* **16**, 129.

FAGE, A. & JOHANSEN, F. C. 1927 On the flow of air behind an inclined flat plate of infinite span. *Proc. Roy. Soc.* A **116**, 170.

GERRARD, J. H. 1966 The mechanics of the formation region of vortices behind bluff bodies. *J. Fluid Mech.* **25**, 401.

GERRARD, J. H. 1967 Numerical computation of the magnitude and frequency of the lift on a circular cylinder. *Phil. Trans. Roy. Soc.* A **211**, 137.

GERRARD, J. H. 1967 Numerical computation of the magnitude and frequency of the lift on a circular cylinder. *Phil. Trans. Roy. Soc.* A **261**, 137.

GOLDSTEIN, S. 1965 *Modern Developments in Fluid Dynamics*, vol. 2. Dover.

KUWAHARA, K. 1973 Numerical study of flow past an inclined flat plate by an inviscid model. *J. Phys. Soc. Japan* **35**, 1545.

LUGT, H. J. & HAUSSLING, H. J. 1974 Laminar flow past an abruptly accelerated elliptic cylinder at 45° incidence. *J. Fluid Mech.* **65**, 711.

SARPKAYA, T. 1975 An inviscid model of two-dimensional vortex shedding for transient and asymptotically steady separated flow over an inclined flat plate. *J. Fluid Mech.* **68**, 109.

TAKAHASHI, T. 1976 Vortex shedding behind two-dimensional bluff bodies in dilute polymer solutions (in Japanese). Graduation thesis, Faculty of Engineering, Hokkaido University.

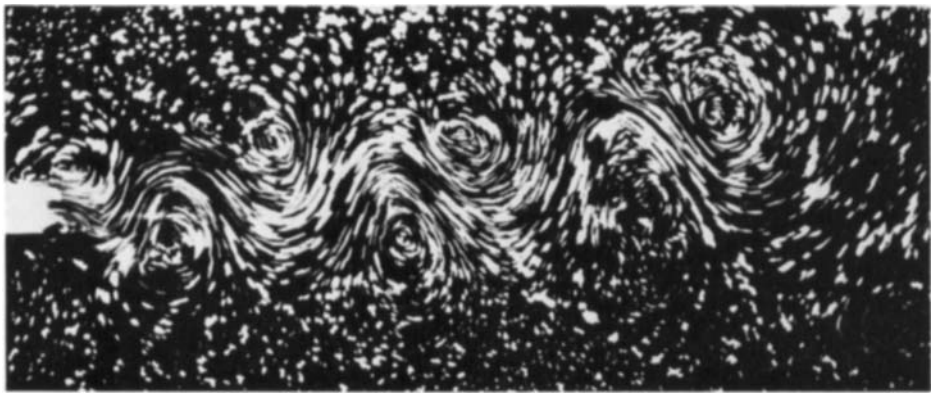

(*a*)

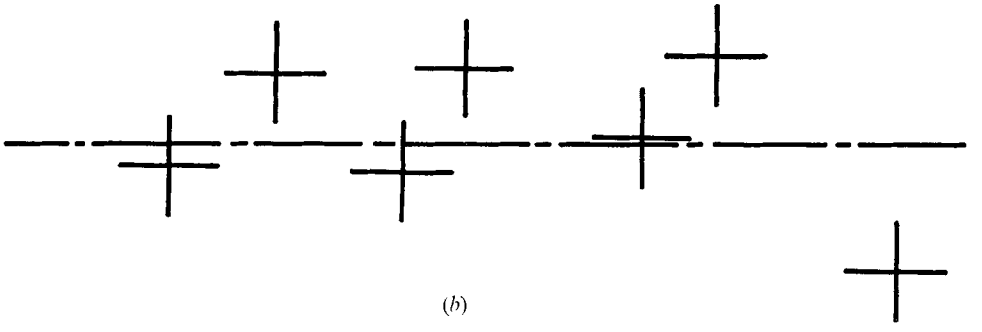

(*b*)

FIGURE 4. (*a*) Photograph of vortex pattern in the wake of a plate set at an angle of attack of 50° at an early stage of flow development; Reynolds number = 1050. (*b*) Approximate locations of the vortices and the free-stream direction. Although the time elapsed since the impulsive start of flow is not identified, the rightmost vortex on the lower side is the first vortex shed into the wake.

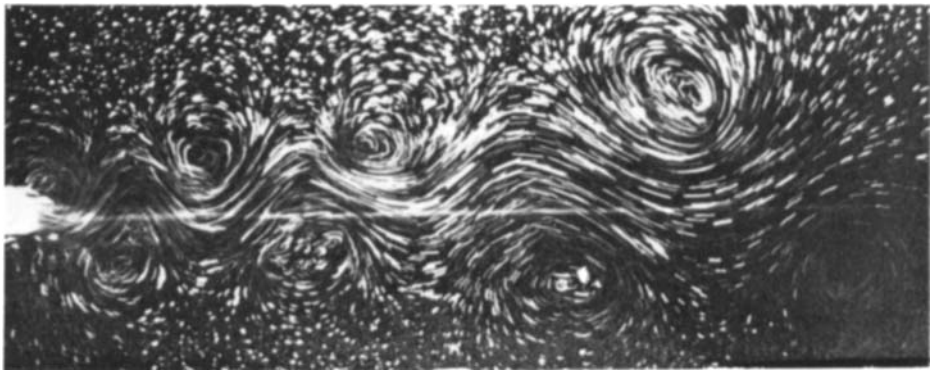

(*a*)

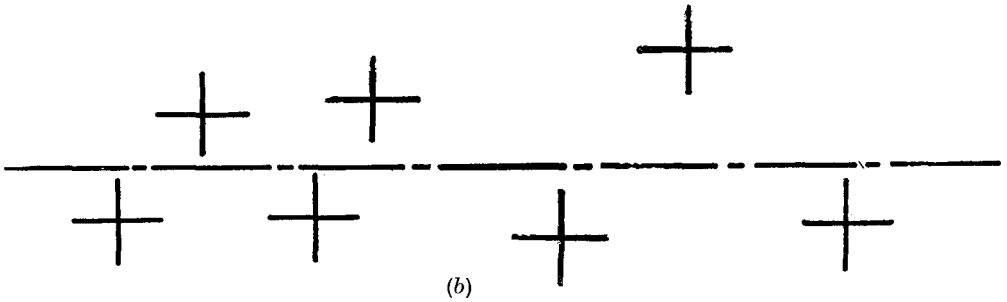

(*b*)

FIGURE 5. (*a*) Photograph of vortex pattern in the wake of a plate set at an angle of attack of 60° at an early stage of flow development; Reynolds number = 2120. (*b*) Approximate locations of the vortices and the free-stream direction. Although the time elapsed since the impulsive start of flow is not identified, the rightmost vortex on the lower side is the first vortex shed into the wake.

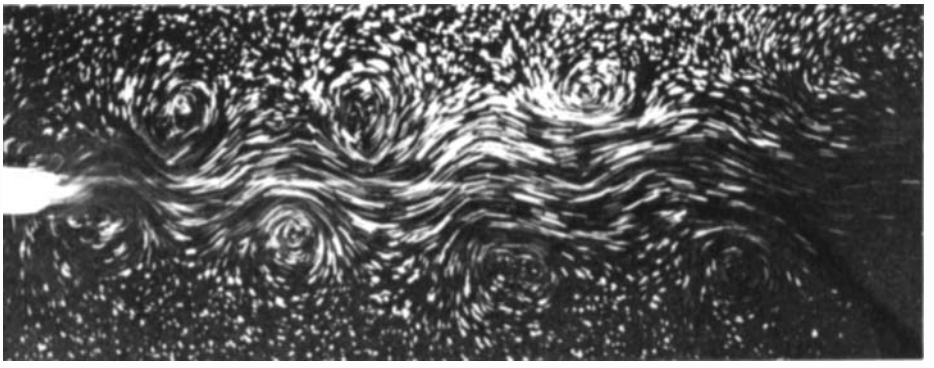

(*a*)

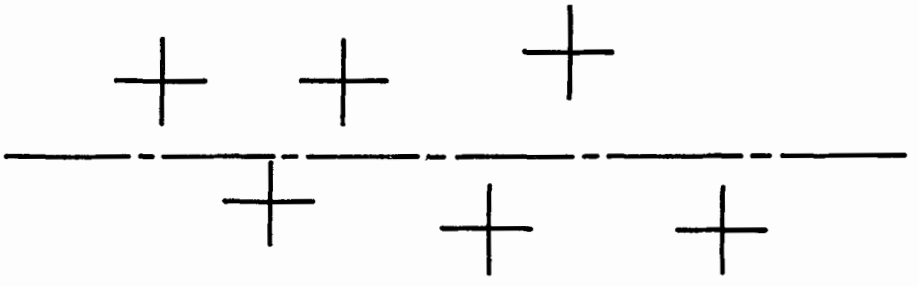

(*b*)

FIGURE 6. (*a*) Photograph of flow pattern in the wake of a plate set at an angle of attack of 60° at the stage of steadily periodic vortex shedding; Reynolds number = 1540. (*b*) Approximate locations of the vortices and the free-stream direction.